

Numerical solution of flame problems with and without multigrid methods

Prof. Craig C. Douglas

University of Kentucky (CS, ME, CCS) and
Yale University (CS)

Dr. Alexandre Ern

CERMICS, ENPC

Prof. Mitchell Smooke

Yale University (ME)

Outline

1. Model Formulation
2. Flame Sheets
 - Problem
 - Discretization
 - Methods
3. Laminar Diffusion Flame with Detailed, Finite Rate Chemistry
 - Problem
 - Methods
4. Parallel Computation
 - Numerical Experiments
5. Conclusions

URL: www.ccs.uky.edu/~douglas

Vorticity–Velocity Formulation

A vorticity-velocity formulation allows replacement of the first order continuity equation with additional second order equations.

Unlike streamfunction-vorticity, vorticity-velocity is extensible to 3D and allows more accurate formulation of boundary conditions in a numerically compact way.

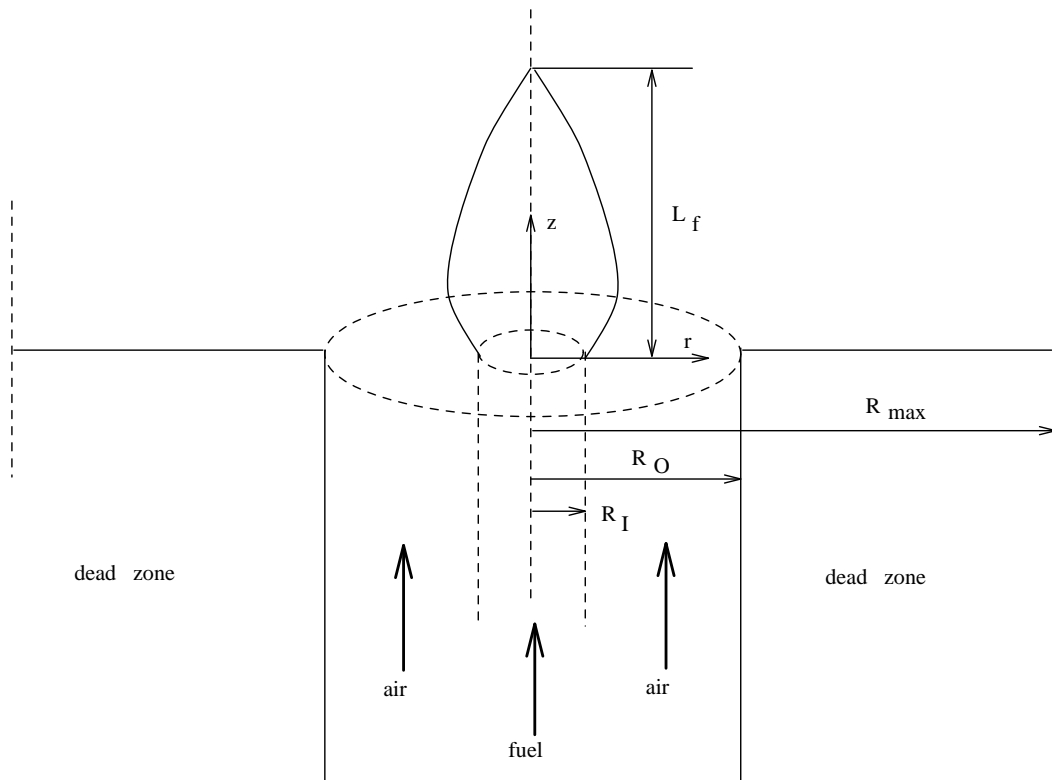
Off diagonal convective terms in off diagonal blocks that exert a strong influence in a streamfunction-vorticity formulation disappear.

Another attractive feature of vorticity-velocity is that the governing equations can be discretized on a nonstaggered grid, thus allowing the implementation of a multigrid algorithm easily.

Flame Sheets

References:

1. C. C. Douglas, A. Ern, and M. D. Smooke, *Numerical simulation of laminar diffusion flames*, in *Applications on Advanced Architecture Computers*, G. Astfalk (ed.), SIAM Books, Philadelphia, 1996, pp. 243–254.
2. C. C. Douglas, A. Ern, and M. D. Smooke, *Multigrid solution of flame sheet problems on serial and parallel computers*, *Parallel Algorithms and Applications*, 10 (1997), pp. 225–236.



Flame Sheet Properties

Used to initialize multidimensional diffusion flames (full chemistry).

Chemical Reactions: one step, irreversible reaction; infinitely fast conversion of reactants into stable products.

Reaction only in exothermic reaction zone located at locus of stoichiometric mixing of fuel and oxidizer; temperature and products of combustion maximized here.

Neglect thermal diffusion effects, assumes constant heat capacities, Frick's law for ordinary mass diffusion velocities, and takes all Lewis numbers equal to unity.

Energy and major chemical species equations take the same form; using Schwab–Zeldovich variables, source free convection–diffusion equation for a single conserved scalar.

No information about minor species; temperature and chemical species profiles can be obtained. Location of reaction zone and temperature distribution can be predicted.

Notation

$v = (v_r, v_z)$	the velocity vector (radial, axial)
$\omega = \frac{\partial v_r}{\partial z} - \frac{\partial v_z}{\partial r}$	the normal component of the vorticity
ρ	the density
μ	the viscosity
g	the gravity vector
$\text{div}(v)$	the cylindrical divergence of the velocity vector
S	the conserved scalar
D	a diffusion coefficient

The components of $\bar{\nabla}\beta$ are $(\frac{\partial\beta}{\partial z}, -\frac{\partial\beta}{\partial r})$.

Governing Equations

The flame sheet governing equations consist of the conservation of total mass, momentum and a conserved scalar equation.

The conservation of total mass and momentum equations constitute the flow field problem and are formulated using the vorticity-velocity formulation of the compressible axisymmetric Navier-Stokes equations.

A source free convective-diffusive equation for a conserved scalar is solved coupled together with the flow field equations and the temperature and major stable species profiles in the system can be recovered from the conserved scalar.

The vorticity transport equation is formed by taking the curl of the momentum equations, which eliminates the partial derivatives of the pressure field. A Laplace equation is obtained for each velocity component by taking the gradient of ω and using the continuity equation. This yields the governing equations in the following form:

$$\frac{\partial^2 v_r}{\partial r^2} + \frac{\partial^2 v_r}{\partial z^2} = \frac{\partial \omega}{\partial z} - \frac{1}{r} \frac{\partial v_r}{\partial r} + \frac{v_r}{r^2} - \frac{\partial}{\partial r} \left(\frac{v \cdot \nabla \rho}{\rho} \right)$$

$$\frac{\partial^2 v_z}{\partial r^2} + \frac{\partial^2 v_z}{\partial z^2} = -\frac{\partial \omega}{\partial r} - \frac{1}{r} \frac{\partial v_r}{\partial z} - \frac{\partial}{\partial z} \left(\frac{v \cdot \nabla \rho}{\rho} \right)$$

$$\frac{\partial^2 \mu \omega}{\partial r^2} + \frac{\partial^2 \mu \omega}{\partial z^2} + \frac{\partial}{\partial r} \left(\frac{\mu \omega}{r} \right) = \rho v_r \frac{\partial \omega}{\partial r} + \rho v_z \frac{\partial \omega}{\partial z} -$$

$$\frac{\rho v_r}{r} \omega + \bar{\nabla} \rho \cdot \nabla \frac{v^2}{2} - \bar{\nabla} \rho \cdot g +$$

$$2 \left(\bar{\nabla}(\text{div}(v)) \cdot \nabla \mu - \nabla v_r \cdot \bar{\nabla} \frac{\partial \mu}{\partial r} - \nabla v_z \cdot \bar{\nabla} \frac{\partial \mu}{\partial z} \right)$$

$$\frac{1}{r} \frac{\partial}{\partial r} (r \rho D \frac{\partial S}{\partial r}) + \frac{\partial}{\partial z} (\rho D \frac{\partial S}{\partial z}) = \rho v_r \frac{\partial S}{\partial r} + \rho v_z \frac{\partial S}{\partial z}$$

Boundary conditions

Axis of symmetry ($r = 0$)

$$v_r = 0, \quad \frac{\partial v_z}{\partial r} = 0,$$

$$\omega = 0, \quad \frac{\partial S}{\partial r} = 0.$$

Outer zone ($r = R_{max}$)

$$\frac{\partial v_r}{\partial r} = 0, \quad \frac{\partial v_z}{\partial r} = 0,$$

$$\omega = \frac{\partial v_r}{\partial z}, \quad S = 0.$$

Inlet ($z = 0$)

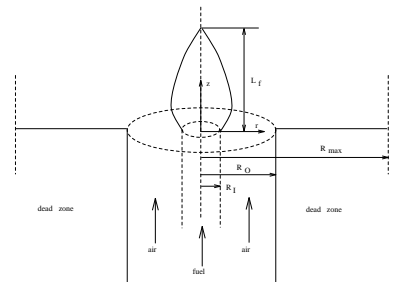
$$v_r = 0, \quad v_z = v_z^0(r),$$

$$\omega = \frac{\partial v_r}{\partial z} - \frac{\partial v_z}{\partial r}, \quad S = S^0(r).$$

Exit ($z = L$)

$$v_r = 0, \quad \frac{\partial v_z}{\partial z} = 0,$$

$$\frac{\partial \omega}{\partial z} = 0, \quad \frac{\partial S}{\partial z} = 0.$$



Discretization

Spatial operators are approximated with finite differences.

Diffusion and source terms are central differenced. Convective terms are upwind differenced to preserve monotonicity.

Most boundary terms are back or forward differenced (1st order). Inlet points and axial boundary conditions 2nd order differenced.

Note: A mixed finite element procedure would probably be better.

Right hand side is evaluated using the Laplace equation for v_z . On the axis of symmetry, this reduces to

$$\frac{\partial^2 v_z}{\partial r^2} = -\frac{\partial^2 v_z}{\partial z^2} - \frac{\partial \omega}{\partial r} - \frac{\partial}{\partial z} \left(\frac{v_z \partial \rho}{\rho \partial z} \right).$$

The discretized PDE + the boundary conditions yields a set of algebraic equations of the form $F(U) = 0$, which is solved using a damped Newton method

$$J(U^n)\Delta U^n = -\lambda^n F(U^n), \quad n = 0, 1, \dots,$$

with convergence tolerance $\|\Delta U^n\|_S < 10^{-q}$ ($q \in \{5, 6\}$). The Jacobian matrix $J(U^n)$ is computed numerically.

Rather than working with dimensionless variables, we introduce scale factors α_l , $l \in [1, n_c]$, for each dependent variable ($n_c = 4$ for the flame sheet problem). The norm of the discrete vector ΔU^n is then given by

$$\|\Delta U^n\|_S = \sqrt{\sum_{\substack{i \in [1, n_r] \\ j \in [1, n_z] \\ l \in [1, n_c]}} (\alpha_l \Delta U^n(l, i, j))^2}.$$

This part is solved with an inner iteration.

Due to the nonlinearity of the original problem, a pseudo transient process is used to produce a parabolic in time problem and bring the starting estimate into the convergence domain of the steady Newton method. The original nonlinear elliptic problem is cast into a parabolic form by appending a pseudo transient term $\frac{\partial U}{\partial t}$ to the original set of algebraic equations $F(U) = 0$, and a fully implicit scheme solves (again with Newton method)

$$\mathcal{F}(U^{n+1}) = F(U^{n+1}) + \frac{U^{n+1} - U^n}{\Delta t^{n+1}} = 0,$$

where Δt^{n+1} is the $(n + 1)^{\text{st}}$ time step.

Multigrid techniques

We assume that there is a sequence of spaces \mathcal{M}_i , $i = 1, \dots, k$, where the \mathcal{M}_i approximate \mathcal{M}_1 . We further suppose there exist *restriction* and *prolongation* mappings

$$\begin{cases} \mathcal{R}_i : \mathcal{M}_i \rightarrow \mathcal{M}_{i+1}, & 1 \leq i \leq k-1, \\ \mathcal{P}_i : \mathcal{M}_i \rightarrow \mathcal{M}_{i-1}, & 2 \leq i \leq k. \end{cases}$$

between neighboring spaces. We also assume there is a sequence of nonlinear problems represented by J_i .

Two multigrid algorithms (correction and nested iteration).

Algorithm MGC ($lev, \{J_j, x_j, b_j\}_{j=1}^k,$
 $\{\mathcal{P}_j\}_{j=2}^k, \{\mathcal{R}_j\}_{j=1}^{k-1}$)

1. $x_{lev} \leftarrow \text{Solver}_{lev}(J_{lev}, x_{lev}, b_{lev})$
2. If $lev < k$, then repeat 2a–2d until some condition is met:
 - 2a. $x_{lev+1} \leftarrow 0,$
 $b_{lev+1} \leftarrow \mathcal{R}_{lev}(b_{lev} - J_{lev}x_{lev})$
 - 2b. MGC ($lev + 1, \{J_j, x_j, b_j\}_{j=1}^k,$
 $\{\mathcal{P}_j\}_{j=2}^k, \{\mathcal{R}_j\}_{j=1}^{k-1}$)
 - 2c. $x_{lev} \leftarrow x_{lev} + \mathcal{P}_{lev+1}x_{lev+1}$
 - 2d. $x_{lev} \leftarrow \text{Solver}_{lev}(J_{lev}, x_{lev}, b_{lev})$

The solver on every level is either

Bi-CGSTAB/GS or GMRES/GS.

- Algorithm NIC ($lev, \{J_j, x_j, b_j\}_{j=1}^k,$
 $\{\mathcal{P}_j\}_{j=2}^k, \{\mathcal{R}_j\}_{j=1}^{k-1}$)
1. MGC ($k, \{J_j, x_j, b_j\}_{j=1}^k, \{\mathcal{P}_j\}_{j=2}^k,$
 $\{\mathcal{R}_j\}_{j=1}^{k-1}$)
 2. Do steps 2a–2b with $lev = k - 1, \dots, 1$:
 - 2a. $x_{lev} \leftarrow \mathcal{P}_{lev+1} x_{lev+1}$
 - 2b. MGC ($lev, \{J_j, x_j, b_j\}_{j=1}^k, \{\mathcal{P}_j\}_{j=2}^k,$
 $\{\mathcal{R}_j\}_{j=1}^{k-1}$)

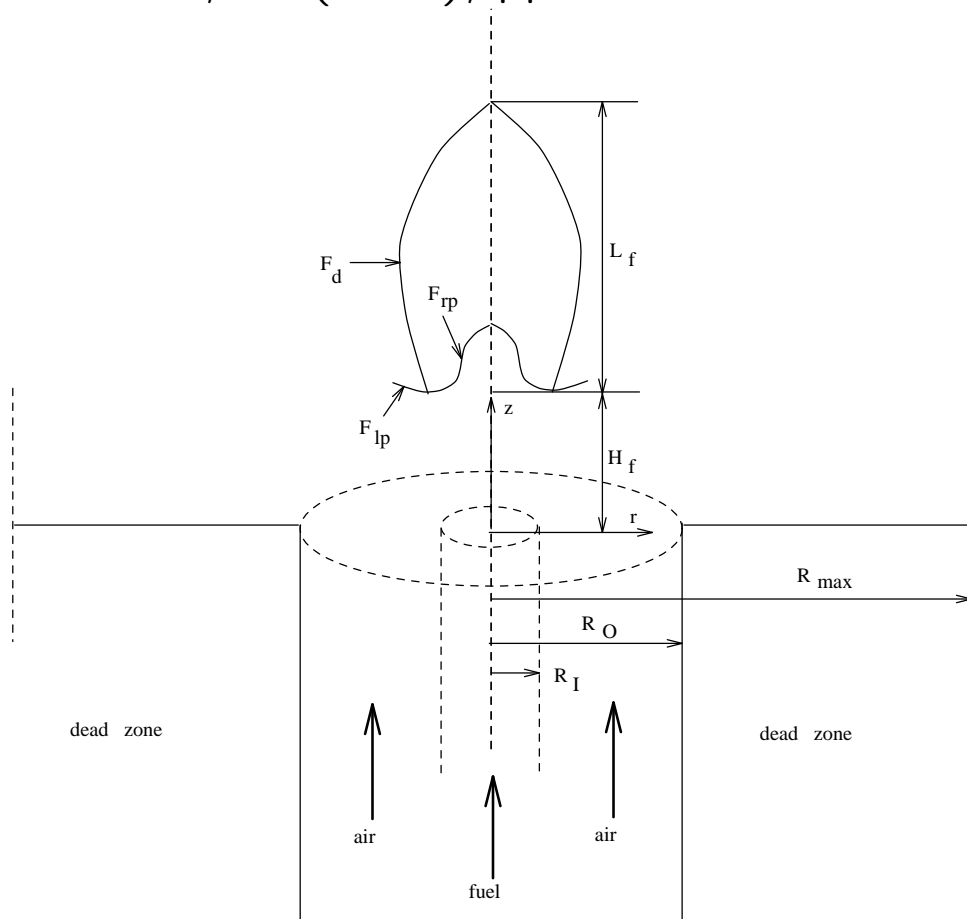
Damped Newton multilevel algorithm: Before each reference to Algorithm MGC in NIC, a Jacobian is formed and a damped Newton step is performed.

One way multilevel algorithm: Algorithm MGC never performs any portion of its step 2 as part of its use by Algorithm NIC.

Laminar Diffusion Flames with Detailed Chemistry

References:

1. A. Ern, C. C. Douglas, and M. D. Smooke, *Detailed chemistry modeling of laminar diffusion flames on parallel computers*, International Journal of Supercomputer Applications and High Performance Computing, 9 (1995), pp. 167–186.
2. C. C. Douglas, A. Ern, and M. D. Smooke, *High performance computing and numerical simulation of flames* ZAMM, 76 (1996), pp. 49–52.



Laminar Diffusion Flame Properties

Physical configuration: inner cylindrical fuel stream surrounded by a coflowing oxidizer jet. Inlet velocities high enough to produce a lifted flame with a triple flame ring structure.

Solve for: total mass, momentum, energy, and chemical species conservation equation.

Numerical solution involves: pseudo transient process, steady state Newton multigrid. Coarse grid information initializes fine grid problems. Flame sheet initializes problem solution.

Variable width tensor product, nested grids. Adaptive grid refinement useful since the area of activity changes as the grids are refined.

Interpolation becomes very important; it is hard to keep solutions in the convergence domain of damped Newton after grid refinements.

Notation

$v = (v_r, v_z)$	the hydrodynamic velocity vector (radial, axial)
$\omega = \frac{\partial v_r}{\partial z} - \frac{\partial v_z}{\partial r}$	the normal component of the vorticity
p	the pressure
ρ	the mass density of the mixture
μ	the shear viscosity
g	the gravity vector
$\text{div}(v)$	the cylindrical divergence of the velocity vector
c_p	the specific constant pressure heat capacity of the mixture
T	the temperature
λ	the thermal conductivity of the mixture

K	the total number of species
c_{pk}	the specific constant pressure heat capacity of the k th species
Y_k	the mass fraction of the k th species
$V_k = (V_{kr}, V_{kz})$	the diffusion velocity of the k th species
h_k	the specific enthalpy of the k th species
W_k	the molecular weight of the k th species
$\dot{\omega}_k$	the molar production rate of the k th species per unit volume
\bar{W}	the mean molecular weight of the mixture
R	the universal gas constant

Governing Equations

Energy:

$$\begin{aligned} \rho c_p v_r \frac{\partial T}{\partial r} + \rho c_p v_z \frac{\partial T}{\partial z} = \\ \frac{1}{r} \frac{\partial}{\partial r} \left(r \lambda \frac{\partial T}{\partial r} \right) + \frac{\partial}{\partial z} \left(\lambda \frac{\partial T}{\partial z} \right) - \\ \sum_{k=1}^K \left[\rho c_{pk} Y_k \left(V_{kr} \frac{\partial T}{\partial r} + V_{kz} \frac{\partial T}{\partial z} \right) \right] - \\ \sum_{k=1}^K h_k W_k \dot{\omega}_k. \end{aligned}$$

Species:

$$\begin{aligned} \rho v_r \frac{\partial Y_k}{\partial r} + \rho v_z \frac{\partial Y_k}{\partial z} = \\ - \frac{1}{r} \frac{\partial}{\partial r} \left(r \rho Y_k V_{kr} \right) - \frac{\partial}{\partial z} \left(\rho Y_k V_{kz} \right) + W_k \dot{\omega}_k, \\ k = 1, \dots, K. \end{aligned}$$

Vorticity–velocity formulation of Navier–Stokes:

$$\frac{\partial^2 v_r}{\partial r^2} + \frac{\partial^2 v_r}{\partial z^2} = \frac{\partial \omega}{\partial z} - \frac{1}{r} \frac{\partial v_r}{\partial r} + \frac{v_r}{r^2} - \frac{\partial}{\partial r} \left(\frac{v \cdot \nabla \rho}{\rho} \right)$$

$$\frac{\partial^2 v_z}{\partial r^2} + \frac{\partial^2 v_z}{\partial z^2} = -\frac{\partial \omega}{\partial r} - \frac{1}{r} \frac{\partial v_r}{\partial z} - \frac{\partial}{\partial z} \left(\frac{v \cdot \nabla \rho}{\rho} \right)$$

$$\frac{\partial^2 \mu \omega}{\partial r^2} + \frac{\partial^2 \mu \omega}{\partial z^2} + \frac{\partial}{\partial r} \left(\frac{\mu \omega}{r} \right) = \rho v_r \frac{\partial \omega}{\partial r} + \rho v_z \frac{\partial \omega}{\partial z} -$$

$$\frac{\rho v_r}{r} \omega + \bar{\nabla} \rho \cdot \nabla \frac{v^2}{2} - \bar{\nabla} \rho \cdot g +$$

$$2 \left(\bar{\nabla}(\text{div}(v)) \cdot \nabla \mu - \nabla v_r \cdot \bar{\nabla} \frac{\partial \mu}{\partial r} - \nabla v_z \cdot \bar{\nabla} \frac{\partial \mu}{\partial z} \right)$$

$$\bar{\nabla} \beta = \left(\frac{\partial \beta}{\partial z}, -\frac{\partial \beta}{\partial r} \right) \text{ for any scalar } \beta.$$

Due to the high temperature gradients present in the system, the viscosity derivatives in the r.h.s. cannot be neglected.

Boundary conditions

Axis of symmetry ($r = 0$)

$$v_r = 0, \quad \frac{\partial v_z}{\partial r} = 0, \quad \frac{\partial Y_k}{\partial r} = 0,$$

$$\omega = 0, \quad \frac{\partial T}{\partial r} = 0.$$

Outer zone ($r = R_{max}$)

$$\frac{\partial v_r}{\partial r} = 0, \quad \frac{\partial v_z}{\partial r} = 0, \quad Y_k = Y_{k_{air}},$$

$$\omega = \frac{\partial v_r}{\partial z}, \quad T = T_{air}.$$

Inlet ($z = 0$)

$$v_r = 0, \quad v_z = v_z^0(r), \quad Y_k = Y_k^0(r),$$

$$\omega = \frac{\partial v_r}{\partial z} - \frac{\partial v_z}{\partial r}, \quad T = T^0(r).$$

Exit ($z = L$)

$$v_r = 0, \quad \frac{\partial v_z}{\partial z} = 0, \quad \frac{\partial Y_k}{\partial z} = 0,$$

$$\frac{\partial \omega}{\partial z} = 0, \quad \frac{\partial T}{\partial z} = 0.$$

Parallel Computation

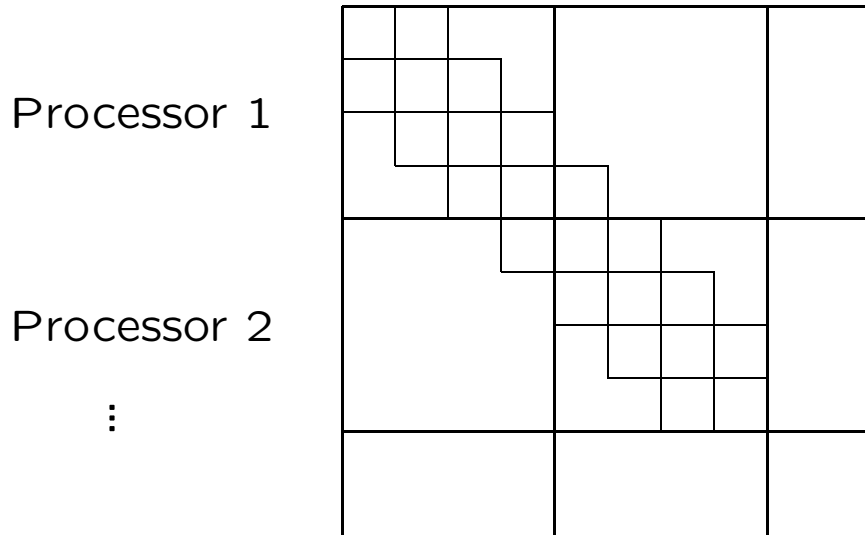
Both the flame sheet and laminar diffusion flame codes have been parallelized. We did not do this just to speed up the codes: we ran out of memory. Even with 128Mb–1Gb per node, we ran out of memory.

The preconditioned matrix iterative solvers, matrix–vector multipliers, nonlinear function evaluations, and Jacobian constructions are all parallelized. Communications is normally minimized.

We use a sparse matrix domain decomposition method (we treat the matrix as a 2D domain) – much more efficient than standard domain decomposition.

A few operations are best done on a single processor. We gather the parts of some vector, do the operation, and then scatter the result vector back. Since the vectors are small with respect to the Jacobians, the extra storage is not noticeable. This is quick and very efficient.

Upper left corner of the Jacobian matrix block structure



This is just a *strip domain decomposition*. It is quite efficient for communications and experience shows that it also effective as a decomposition method.

The connecting blocks contain some subblocks which are completely zero, which we take advantage of. This is due to the boundary conditions.

Flame Sheet Numerical Results

Grids:

129 × 161 finest level

...

17 × 21 coarsest level

Jacobians are 36 point operators (4 components per grid point, 9 point discretization).

Three sets of numbers:

1. Pseudo transient phase (coarse level only).
2. One way nonlinear multigrid.
3. Damped Newton multigrid.

Two solvers:

1. Bi-CGSTAB/GS
2. GMRES/GS

Numerical results for one way nonlinear multi-grid during the time relaxation phase

Operation	Levels			
	1	2	3	4
Bi-CGSTAB/GS				
CPU minutes	41.5	6.3	1.2	0.25
Speedup	1.0	6.6	34.6	166.0
GMRES/GS				
CPU minutes	—	5.8	1.2	0.26
Speedup	—	7.2	34.6	159.6

The speedups are with respect to the unilevel solution time (41.5mn) and the CPU minutes measures 20 time steps.

Time reduced from many, many minutes to a few seconds on a workstation.

Numerical results for one way nonlinear multi-grid

Operation	Levels			
	1	2	3	4
Bi-CGSTAB/GS				
CPU minutes	96.2	22.9	17.7	16.5
Speedup	1.0	4.2	5.4	5.8
GMRES/GS				
CPU minutes	—	29.7	23.0	23.1
Speedup	—	3.2	4.2	4.2

The speedups are with respect to the unilevel solution time (96.2mn).

Storage = 39 Mb

Numerical results for damped Newton multi-level iterations

Operation	Levels			
	1	2	3	4
Bi-CGSTAB/GS				
CPU minutes	96.2	20.4	15.7	14.7
Speedup	1.0	4.8	6.2	6.6
GMRES/GS				
CPU minutes	—	19.0	9.7	9.2
Speedup	—	5.1	9.9	10.5

The speedups are with respect to the unilevel solution time (96.2mn).

Storage = 62 Mb

Numerical results for parallel iterations on an IBM SP2

One way multilevel				
Operation	Processors			
	1	2	4	8
Bi-CGSTAB/GS				
CPU minutes	4.26	2.30	1.26	0.77
Speedup	1.0	1.8	3.4	5.5
GMRES/GS				
CPU minutes	6.32	3.31	1.84	1.09
Speedup	1.0	1.9	3.4	5.8
Damped Newton multilevel				
Bi-CGSTAB/GS				
CPU minutes	4.57	2.58	1.20	0.77
Speedup	1.0	1.8	3.8	5.9
GMRES/GS				
CPU minutes	5.20	2.59	1.35	0.86
Speedup	1.0	2.0	3.8	6.0

Four levels were used in each run.

Laminar Diffusion Numerical Results

Flame configuration: methane–air lifted laminar diffusion flame with a triple flame structure at its base. This was chosen since we have experimental results for it.

The numerical solution includes 16 chemical species engaged in a C1-chain reaction mechanism, i.e., only molecules with at most *one* carbon atom are considered. Additionally, there are four unknowns associated with each mesh point for a total of 20 unknowns per mesh point.

The flame is appropriately resolved with 5×10^3 mesh nodes, and very good agreement with previous experimental (2.5×10^5 data points) data is obtained.

C₁-Chain Methane-Air Reaction Mechanism

Rate coefficients: $k^F = AT^\beta \exp(-E/RT)$

(units: moles, cubic centimeters, seconds, Kelvins and calories)

Reaction	A	β	E
1. CH ₃ +H \rightleftharpoons CH ₄	1.90E+36	-7.000	9050.
2. CH ₄ +O ₂ \rightleftharpoons CH ₃ +HO ₂	7.90E+13	0.000	56000.
3. CH ₄ +H \rightleftharpoons CH ₃ +H ₂	2.20E+04	3.000	8750.
4. CH ₄ +O \rightleftharpoons CH ₃ +OH	1.60E+06	2.360	7400.
5. CH ₄ +OH \rightleftharpoons CH ₃ +H ₂ O	1.60E+06	2.100	2460.
6. CH ₂ O+OH \rightleftharpoons HCO+H ₂ O	7.53E+12	0.000	167.
7. CH ₂ O+H \rightleftharpoons HCO+H ₂	3.31E+14	0.000	10500.
8. CH ₂ O+M \rightleftharpoons HCO+H+M	3.31E+16	0.000	81000.
9. CH ₂ O+O \rightleftharpoons HCO+OH	1.81E+13	0.000	3082.
10. HCO+OH \rightleftharpoons CO+H ₂ O	5.00E+12	0.000	0.
11. HCO+M \rightleftharpoons H+CO+M	1.60E+14	0.000	14700.
12. HCO+H \rightleftharpoons CO+H ₂	4.00E+13	0.000	0.
13. HCO+O \rightleftharpoons OH+CO	1.00E+13	0.000	0.
14. HCO+O ₂ \rightleftharpoons HO ₂ +CO	3.00E+12	0.000	0.
15. CO+O+M \rightleftharpoons CO ₂ +M	3.20E+13	0.000	-4200.
16. CO+OH \rightleftharpoons CO ₂ +H	1.51E+07	1.300	-758.
17. CO+O ₂ \rightleftharpoons CO ₂ +O	1.60E+13	0.000	41000.
18. CH ₃ +O ₂ \rightleftharpoons CH ₃ O+O	7.00E+12	0.000	25652.
19. CH ₃ O+M \rightleftharpoons CH ₂ O+H+M	2.40E+13	0.000	28812.
20. CH ₃ O+H \rightleftharpoons CH ₂ O+H ₂	2.00E+13	0.000	0.
21. CH ₃ O+OH \rightleftharpoons CH ₂ O+H ₂ O	1.00E+13	0.000	0.
22. CH ₃ O+O \rightleftharpoons CH ₂ O+OH	1.00E+13	0.000	0.
23. CH ₃ O+O ₂ \rightleftharpoons CH ₂ O+HO ₂	6.30E+10	0.000	2600.
24. CH ₃ +O ₂ \rightleftharpoons CH ₂ O+OH	5.20E+13	0.000	34574.
25. CH ₃ +O \rightleftharpoons CH ₂ O+H	6.80E+13	0.000	0.
26. CH ₃ +OH \rightleftharpoons CH ₂ O+H ₂	7.50E+12	0.000	0.
27. HO ₂ +CO \rightleftharpoons CO ₂ +OH	5.80E+13	0.000	22934.
28. H ₂ +O ₂ \rightleftharpoons 2OH	1.70E+13	0.000	47780.
29. OH+H ₂ \rightleftharpoons H ₂ O+H	1.17E+09	1.300	3626.
30. H+O ₂ \rightleftharpoons OH+O	2.00E+14	0.000	16800.
31. O+H ₂ \rightleftharpoons OH+H	1.80E+10	1.000	8826.
32. H+O ₂ +M \rightleftharpoons HO ₂ +M ^a	2.10E+18	-1.000	0.
33. H+O ₂ +O ₂ \rightleftharpoons HO ₂ +O ₂	6.70E+19	-1.420	0.
34. H+O ₂ +N ₂ \rightleftharpoons HO ₂ +N ₂	6.70E+19	-1.420	0.
35. OH+HO ₂ \rightleftharpoons H ₂ O+O ₂	5.00E+13	0.000	1000.
36. H+HO ₂ \rightleftharpoons 2OH	2.50E+14	0.000	1900.
37. O+HO ₂ \rightleftharpoons O ₂ +OH	4.80E+13	0.000	1000.
38. 2OH \rightleftharpoons O+H ₂ O	6.00E+08	1.300	0.
39. H ₂ +M \rightleftharpoons H+H+M ^b	2.23E+12	0.500	92600.
40. O ₂ +M \rightleftharpoons O+O+M	1.85E+11	0.500	95560.
41. H+OH+M \rightleftharpoons H ₂ O+M	7.50E+23	-2.600	0.
42. H+HO ₂ \rightleftharpoons H ₂ +O ₂	2.50E+13	0.000	700.
43. HO ₂ +HO ₂ \rightleftharpoons H ₂ O ₂ +O ₂	2.00E+12	0.000	0.
44. H ₂ O ₂ +M \rightleftharpoons OH+OH+M	1.30E+17	0.000	45500.
45. H ₂ O ₂ +H \rightleftharpoons HO ₂ +H ₂	1.60E+12	0.000	3800.
46. H ₂ O ₂ +OH \rightleftharpoons H ₂ O+HO ₂	1.00E+13	0.000	1800.

Third body efficiencies: ^a H₂O = 21, CO₂ = 5, H₂ = 3.3, CO=2, N₂=O₂ = 0.

^b H₂O = 6, H = 2, H₂ = 3.

Consider a one-way nonlinear multigrid method with Bi-CGSTAB/GS as the solver on all levels. On the finest level, the wall-clock times for convergence on the 89×85 grid are given below.

Machine	Procs.	Wall Time	Speedup
RS6000-580	1	602.59	1.00
SP1	4	137.21	4.39
	8	70.37	8.56
	12	58.89	10.23
	16	53.85	11.19
SP2	8	40.10	15.03
	16	20.96	28.75

Peak speeds:

Mflops	Machine
130	SP1 and RS6000-580
266	SP2 (wide node)

Put the pretty pictures here

Conclusions

The governing equations use the vorticity-velocity formulation of the Navier-Stokes equations coupled together with an energy and the species mass conservation equations.

The results are obtained on a nonstaggered grid and the numerical solution is in very good agreement with previous numerical and experimental data.

A nonlinear damped Newton multigrid procedure yields significant savings in the execution times and fast convergence rates. Solution times on parallel computers reduced solution times from days to minutes.

For three dimensional problems using parallel computers, we should obtain speedups much greater than 10.